Multi-Beam Arrays for Future LEO SatCom Payloads

# Multi-beam arrays for future LEO SatCom payloads

Carlos Vazquez-Sogorb*, Roger Montoya-Roca*, Giuseppe Addamo*, Oscar Peverini*, Giuseppe Virone*
*IEIIT, National Research Council of Italy - CNR, Turin, Italy, carlos.vazquezsogorb@ieiit.cnr.it

***Abstract*—LEO satellite antennas must provide several beams at the same time up to Ka-band over a large scanning angle (up to $\pm 60^{\circ}$). For this reason, high performance radiating elements and beamforming circuitry becomes crucial for the development of new constellations. This paper outlines the challenges and limitations of both waveguide-based and Vivaldi-based solutions and their impact on the beam-formed patterns.**

***Index Terms*—Satellite communication, Phased array, BFN, Waveguide, Vivaldi.**

## I. Introduction

More and more applications require real uninterrupted connectivity and worldwide coverage [1]. In the 6G framework, the integration of terrestrial and Non-Terrestrial Networks (NTN) is well known as a promising solution. GEO and MEO satellites have been used to enhance the coverage on the Earth and to provide a backhaul link when the terrestrial network is not operating. Nevertheless, they are located at high orbits where low latency is not feasible due to the long propagation path [2]. Accordingly, LEO satellite communication has emerged as a promising solution which allows low latency data transfer due to its low altitudes, raising the need for the development of radio-frequency devices in the millimeter and sub-millimeter bands [3].

LEO satellites demands phased array antennas which could provide tens of simultaneous beams to support multiple users. Furthermore, LEO satellite antennas requires to have a high scanning angle (up to $\pm 60^{\circ}$) to provide connectivity in large areas. Nowadays, Direct Radiating Arrays (DRA) are selected for LEO satellite antennas since they permit small size, low cost and lightweight. Such structures are of great interest in fixed ground-based terminals and radar systems as well [4].

The circuitry exployed for steering the beams through controlling the excitation of each element in the array is the beamforming network (BFN). So far, analog BFN have been used for their low cost and power consumption [5]. Nowadays, full digital BFN has emerged as an alternative providing better performance in terms of the number of beams generated. However, it is still not feasible due to its high cost and power consumption [6]. For this reason, hybrid BFN (analog & digital) is currently being adopted as the most promising BFN providing a good balance between energy consumption, cost and an overall higher performance [7].

All the beamforming hardware solution requires proper calibration to achieve the required performance. In this work, we will start analyzing the impact of the non-idealities of the radiating elements on the array beam performance with the aim of identifying possible improvements that can be achieved by suitable calibration/correction procedures.

## II. Multi Beam architecture

The design of a BFN architecture is determined by the specifications of the overall system, such as the number of radiating elements and the number of beams. For a 48x48 element planar array and four steering beams, a possible analog architecture is shown in Fig. 1.

Starting the description of the architecture from the radiating elements, these are directly connected to a High Power Amplifier (HPA). The beamformer (BF) stage is located before the HPA. The present architecture is based on a commercial device from Analog Devices (ADAR3000) which has four inputs and four outputs (i.e 16 beamforming channels). These four inputs correspond to the desired beams. If we repeat the above scheme twelve times in parallel, adding also four 1:12 splitters, we obtain all the elements necessary to form a row of 48 radiating elements. Finally, to make a planar array, we have to replicate the above scheme 48 times in parallel, also adding four 1:48 dividers. In this way, the different beams are distributed equally to all the BFs involved.

This type of architecture has been particularized for a single polarization. During the conference, the scaling to dual polarization and more beams will be shown, where the structural complexity due to the increase of ports in radiating elements and combiners/splitters will be reflected. Hybrid configuration can be proposed by substituting the dividers with multiples RF chains that are fed by digital signals.

## III. Array element

Antennas made of metallic material turn out to be the most reliable option for satellite communication payloads due to their low losses and high power capability [10]. In this context, a square waveguide loaded with ridges, called quadridge, and all-metal Vivaldi (Fig. 2) are proposed. Their designs have been optimized for Ka-downlink band operation in terms of Active Reflection Coefficient [11]. In the case of the quadridge, the thickness of the metal walls is 0.5 mm with a width and height of the ridges of 1 mm and 1.5 mm, respectively. Concerning the Vivaldi, the thickness of the flares is 1 mm, with a total height of 10 mm and containing a cavity with radius of 1.5 mm. In this work, we instead present some results about the scan loss and cross-polarization to assess the impact on the array pattern.

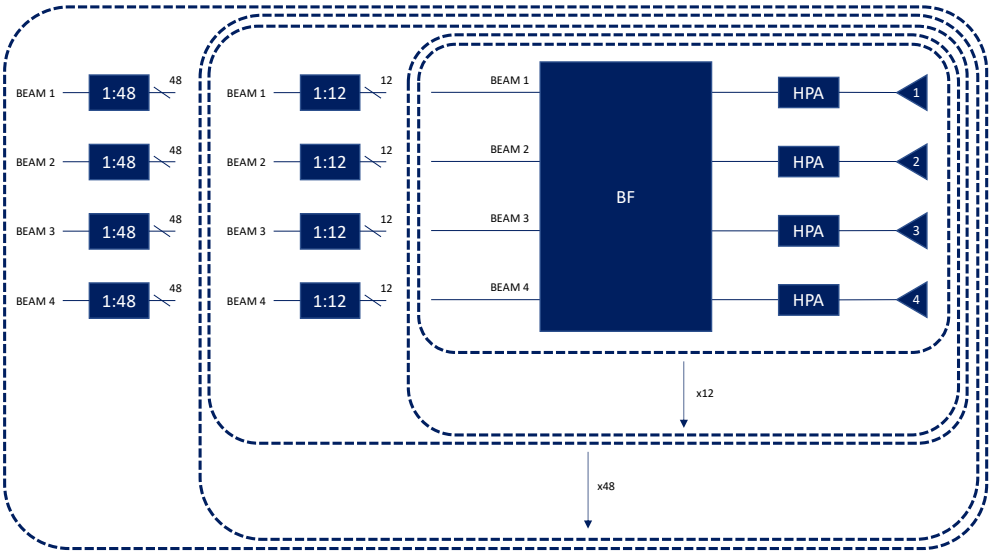


Fig. 1: Example of multi-beam analog BFN architecture for 48x48 planar array

CST software with unit cell boundary conditions has been applied for both designs. In both cases the Active Element Pattern (AEP) is calculated using an infinite array approach and the array scanning method. In the case of the quadridge, the excitation is performed with a waveguide port, while in the case of the Vivaldi, it is performed with two discrete ports, one for each flare. Fig. 3 shows E and H planes at three frequencies in the operating Ka-downlink band for both configurations. Although this kind of antennas works in circular polarization [12], at this level of the study, linear polarization patterns have been considered to avoid additional post-processing on the simulated data.

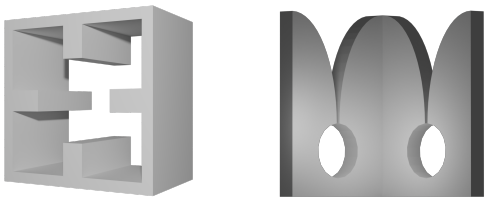

(a) Quadridge (b) All-metal Vivaldi

Fig. 2: Proposed antennas

The quadridge design shows better behaviour at low frequencies of the band, worsening its performance in both planes as the frequency increases. The 3 dB Field of View (FoV) is $\pm 60°$ at lower limit of the band. At central frequency FoV is reduced to 55° for the H-plane. For the upper limit of the band, FoV is reduced to 35° and 50° for the E and H planes, respectively. This decrease in the E-plane is due to the scan blindness suffered at the high frequency of the band when scanning up to the designed limit.

The performance of the Vivaldi mainly remains constant at all frequencies for both planes. The E-plane 3 dB FoV reach

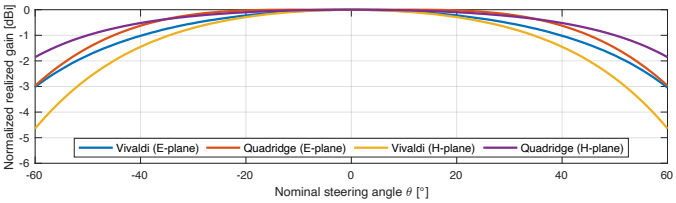


(a) f = 17.7 GHz

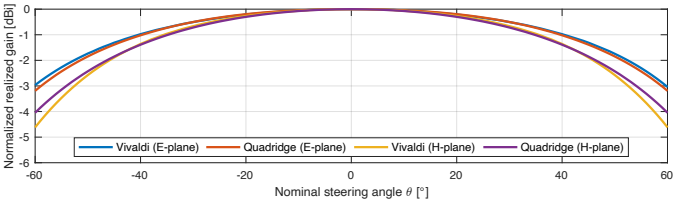


(b) f = 19 GHz

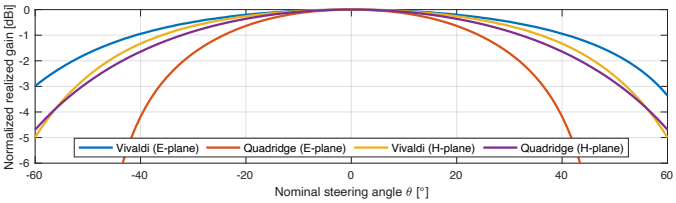


(c) f = 20.2 GHz

Fig. 3: AEP comparison between antennas at E and H planes

60°, while in the H-plane it is limited to about 50°. The scan loss at 60° is within 5 dB.

As far as cross-polarization performance is concerned, Fig. 4 shows the Co-Pol and Cross-Pol at D-plane for the Vivaldi solution. It is well known that Vivaldi antennas suffer severe cross-polarization in the non-principal plane. This degradation is linked directly with the ratio of element height over

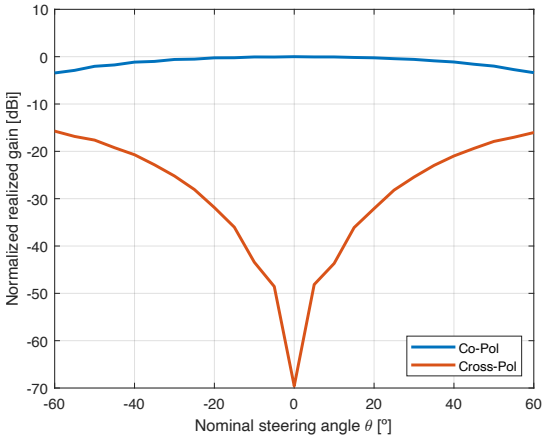


Fig. 4: Co/Cross polarization at 19 GHz at D-plane

element width [13]. The width dimension (7.8 mm) comes from the grating lobe condition in order to avoid them inside the FoV. In this work the height has been kept to low values (10 mm) to achieve acceptable levels of 12 dB of XPD at 60°.

It is difficult to further improve the XPD of the element for this configuration [14]. Possible improvements that could be achieved by beamforming strategies at both element and beam levels will be presented at the conference.

## IV. Impact on the Array Performance

The radiation pattern for a 48x48 array (array size 38x38 $cm^2$) has been simulated using the AEP shown in section 3. This number of elements provides a gain of about 36 dBi. For example, Fig. 5 shows 13 beams separated of 10° for the E-Plane of the Vivaldi solution only. The sidelobe level are close to -13.6 dB because the amplitude distribution is uniform. The computed Full Half Power Beamwidth (FHPBW) and pointing error are shown in Fig. 6 and Fig. 7, respectively.

The FHPBW is equal to 2.3°, 2.15° and 2° at boresight for lower limit, central and upper limit frequencies, respectively. As the scanning angle increases, the FHPBW reaches values 4.5°, 4.2° and 3.8°. At system level, the increase of the FHPBW produces an enlargement of the footprint on Earth. A constant footprint vs. scan angle could be achieved by amplitude tapering. This approach will enlarge the FHPBW for low scanning angles also improving sidelobe levels.

Concerning the pointing error, Fig. 7 shows maximum values of about 0.1° and 0.2° for E-plane and H-plane, respectively, at 60° scan angle. This error is due to the slope of the AEPs which increases towards 60° (Fig. 3). Such error values are less than 10% of the FHPBW, therefore, they are not expected to have strong effect at system level. Nevertheless, the data in Fig. 7 could be used as a calibration table to provide the corrected steering vector at the beamformer. Similar considerations applies to the quadridge element.

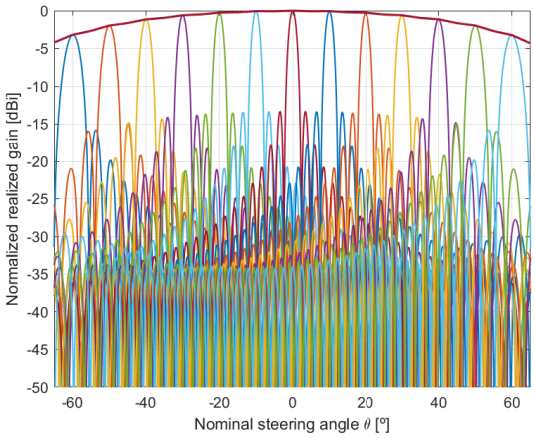


Fig. 5: Simulated scanning radiation pattern at 19 GHz at E-plane for an array of 48x48 elements

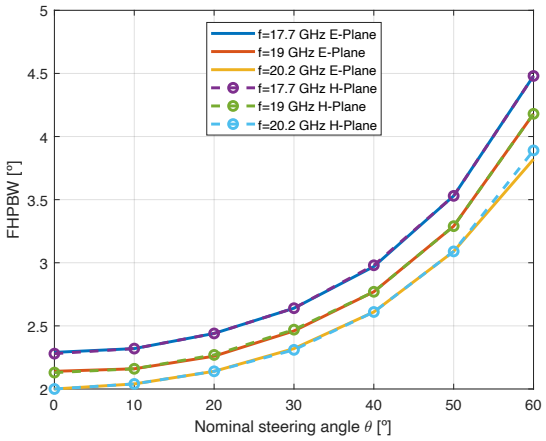


Fig. 6: FHPBW

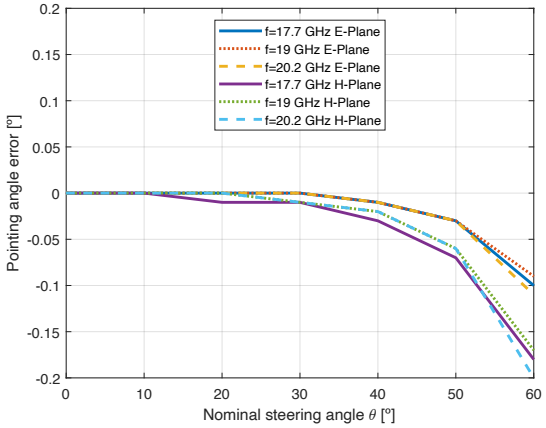


Fig. 7: Pointing error

## V. Conclusion

This paper outlines a multi-beam architecture for LEO satellite payloads. Two radiating elements have been presented comparing their scan loss up to $\pm 60^{\circ}$ and discussing the cross-polarization at D-Plane. The FHPBW and pointing direction error have been analyzed for a 48x48 array. Calibration solutions to improve the overall performance have been envisaged.

## Acknowledgment

Funded by the European Union, under ANTERRA 101072363 HORIZON-MSCA-2021-DN-01. Views and opinions expressed are however those of the author(s) only and do not necessarily reflect those of the European Union. Neither the European Union nor the granting authority can be held responsible for them.

## References

[1] F. Rinaldi et al., "Non-Terrestrial Networks in 5G & Beyond: A Survey," in IEEE Access, vol. 8, pp. 165178-165200, 2020, doi: 10.1109/ACCESS.2020.3022981.

[2] F. Vatalaro, G. E. Corazza, C. Caini and C. Ferrarelli, "Analysis of LEO, MEO, and GEO global mobile satellite systems in the presence of interference and fading," in IEEE Journal on Selected Areas in Communications, vol. 13, no. 2, pp. 291-300, Feb. 1995, doi: 10.1109/49.345873.

[3] H. Kähkönen, J. Ala-Laurinaho and V. Viikari, "Dual-Polarized Ka-Band Vivaldi Antenna Array," in IEEE Transactions on Antennas and Propagation, vol. 68, no. 4, pp. 2675-2683, April 2020, doi: 10.1109/TAP.2019.2948561.

[4] F. Filice, N. Nachabe, C. Luxey and F. Gianesello, "3D-Printed Double-Ridged Waveguide Array Antenna targeting High-Efficiency Ku-band SatCom on The Move Applications," 2019 USNC-URSI Radio Science Meeting (Joint with AP-S Symposium), Atlanta, GA, USA, 2019, pp. 17-18, doi: 10.1109/USNC-URSI.2019.8861755.

[5] D. L. Lemes, M. V. T. Heckler and A. Winterstein, "A low-cost modular transmit front-end with analog beamforming capability," 2017 SBMO/IEEE MTT-S International Microwave and Optoelectronics Conference (IMOC), Aguas de Lindoia, Brazil, 2017, pp. 1-5, doi: 10.1109/IMOC.2017.8121119.

[6] P. K. Bailleul, "A New Era in Elemental Digital Beamforming for Spaceborne Communications Phased Arrays," in Proceedings of the IEEE, vol. 104, no. 3, pp. 623-632, March 2016, doi: 10.1109/JPROC.2015.2511661.

[7] A. Kharalkar, A. Batabyal, R. Zele and S. Gupta, "A Review of Phased-Array Receiver Architectures for 5G Communications," 2022 IEEE Region 10 Symposium (TENSYMP), Mumbai, India, 2022, pp. 1-6, doi: 10.1109/TENSYMP54529.2022.9864369.

[8] P. Uhlig, A. Friedrich, U. Lewark and O. Litschke, "Brick or Tile? Evaluation of Integration Concepts for Microwave Phased Array Antennas," 2020 IEEE 8th Electronics System-Integration Technology Conference (ESTC), Tønsberg, Norway, 2020, pp. 1-5, doi: 10.1109/ESTC48849.2020.9229703.

[9] T. Chaloun et al., "Electronically Steerable Antennas for Future Heterogeneous Communication Networks: Review and Perspectives," in IEEE Journal of Microwaves, vol. 2, no. 4, pp. 545-581, Oct. 2022, doi: 10.1109/JMW.2022.3202626.

[10] Pozar, D. M. (2005). Microwave engineering; 3rd ed. Wiley.

[11] R. Montoya-Roca, C. Vazquez-Sogorb, G. Virone and G. Addamo, "Array Elements for LEO SatCom Payloads," 2023 IEEE Conference on Antenna Measurements and Applications (CAMA), Genoa, Italy, 2023, pp. 453-456, doi: 10.1109/CAMA57522.2023.10352795.

[12] L. Polo-López, E. Menargues, S. Capdevila, G. Toso and M. García-Vigueras, "Solving Sub-Wavelength Lattice Reduction in Full-Metal Front-Ends for Dual-Polarized Active Antennas," in IEEE Transactions on Antennas and Propagation, vol. 70, no. 9, pp. 7413-7426, Sept. 2022, doi: 10.1109/TAP.2022.3198512.

[13] R. Kindt and D. Taylor, "Polarization correction in dual-polarized phased arrays of flared notches," 2011 IEEE International Symposium on Antennas and Propagation (APSURSI), Spokane, WA, USA, 2011, pp. 1961-1964, doi: 10.1109/APS.2011.5996888.

[14] J. T. Logan, R. W. Kindt and M. N. Vouvakis, "Low Cross-Polarization Vivaldi Arrays," in IEEE Transactions on Antennas and Propagation, vol. 66, no. 4, pp. 1827-1837, April 2018, doi: 10.1109/TAP.2018.2809492.